



OPEN ACCESS

Online ISSN: 2353-0391

Algerian Journal of Natural Products

www.univ-bejaia.dz/ajnp

Type of the Paper (Article)

## Isolation and Characterisation of Some Microalgae Bioactive Molecules

\*Emeka Ugoala, George Ndukwe<sup>1</sup>, Rachael Ayo<sup>2</sup>

Fisheries Products' Development Programme, National Institute for Freshwater Fisheries Research,  
P.M.B. 6006, New Bussa 913003, Niger State

<sup>1</sup>Department of Chemistry, Faculty of Science, Ahmadu Bello University, Zaria

<sup>2</sup>Samaru College of Agriculture, Division of Agricultural Colleges, Ahmadu Bello University, Zaria

\* Corresponding author: nnaemekaugoala@gmail.com

Received: 08/06/2016

/Accepted: 31/10/2016 DOI: 10.5281/zenodo.200210

**Abstract:** This study involved the isolation, structure elucidation, and biological screening of secondary metabolites in freshwater microalgae for bioactive and chemically novel compounds. Isolates were fractionated and purified from the methanol, ethyl acetate, dichloromethane, petroleum ether and aqueous extracts of microalgae via column chromatography technique over silica gel using a gradient mixture of solvents. The chemical structures of isolated compounds have been elucidated using Solid-state cross polarization (CP) and magic angle spinning (MAS) <sup>13</sup>C-NMR spectroscopic technique at spectrometer frequency at a field strength corresponding to 91.3695 MHz for <sup>13</sup>C and 363.331 MHz for <sup>1</sup>H. Of the nine compounds isolated, eight have a glycan skeleton with attached amino acids units. Two of the eight contain beta amino acids units. These are not very common metabolites but hold promise as drug leads. The elements of diversity in the isolates were the gluco and manno configurations of the pyranose ring, the  $\alpha$ -configurations at the anomeric centre, and the positions of the carbohydrate and amino acid sectors in the ring. These molecules are not easily available through gene technology since they are post translational products resulting from the activity of glycosyl hydrolases and transferases. The chemical shifts were rationalized in terms of the number of sugar residues, the sugar ring structures, the positions and anomeric configurations of the inter-sugar linkages. Considering all the NMR data, it was concluded that the compounds were glycyglycyglycylglycine,  $\alpha$ -D-glucopyranosyl-2-amino-4-methylpentanoic acid,  $\alpha$ -D-glucopyranosyl-2-methylamino-4-methylpentanoic acid,  $\alpha$ -D-glucopyranosyl-2-amino-4-methylpentanoate,  $\alpha$ -D-glucopyranosyl-glycyglycine,  $\alpha$ -D-glucopyranosyl-3-aminobutanoic acid,  $\alpha$ -D-glucopyranosyl-2,4,7-triaminoctantrioic acid,  $\alpha$ -D-mannopyranosyl-2-amino-3-methylbutanoic acid and  $\alpha$ -D-mannopyranosyl-3-aminobutanoic acid.

**Keywords:** Solid-state NMR, CP/MAS, Glycoamino acids, Carbohydrate, Chemical shift, Carbon resonance

### 1.1. Introduction

Aquaculture in Nigeria as in most West African countries is a mono-commodity industry. This negates value chains and lowers aquaculture competitiveness in both domestic and foreign markets. In livelihood issues, the engagement in more than one economic activity, can improve

the income generations ability of households. By extension, the utilisation of waste-streams from aquaculture operations might yield useful compounds with wide range of applications and as well reduce to the barest minimum the problems of wastages and output under utilisation thus improving the profitability of overall enterprises in order to generate new production and distribution systems, as well as new consumption patterns. Aquaculture waste-streams are secondary or incidental materials that result from aquaculture activities. They include wild caught fish or parts thereof that are not used for human consumption, and materials (e.g. heads, frames and trimmings) generated from processing wild and farmed fish for human consumption, as well as mortalities from fish farms. It also includes phytoplanktons and zooplanktons which are left after the harvest. Adding value to aquaculture byproducts or wastes implies total resource use, meaning that the byproducts or wastes are used as raw materials.

Aquaculture waste-streams represent a huge unexplored resource and harbour a tremendous variety of compounds. Fisheries wastes have tremendous prospects for the production of diversified products like pearl essence, isinglass, fish leather, glue and gelatine etc. which are having immense industrial and market value. Biomedical products from wastes derived from the fish-processing industry (e.g. skin, bones and fins) are attracting considerable attention from industry. Carotenoids and astaxanthins are pigments that can be extracted from crustacean wastes. Fish silage and fish protein hydrolysates obtained from fish viscera are finding applications in the pet feed and the fish feed industries. Another approach being researched is fisheries processing discarded materials, which contains a wealth of potentially valuable biomolecules such as proteins, lipids, enzymes, glucosaminoglycans, vitamins and minerals. Once extracted and stabilised, these molecules can have applications in a wide range of products and processes, from food and nutraceuticals to cosmetics and industrial processing aids.

Microalgae are potentially prolific sources of highly bioactive secondary metabolites with high complexities and unlimited diversity of pharmacological and/or biological properties. Most commercial cultivation of microalgae is currently done in open cultivation ponds. Although these culture ponds are very simple and cheap to construct, in most species their production is very low because they are sensitive to environmental factors and easily contaminated. Consequently, only very few microalgae species that have selective growth condition are currently cultivated on commercial scale [1]. But many microalgae species can be induced to accumulate substantial contents of lipids and bioactive compounds through the use of bioreactors, heterotrophic and mixotrophic cultures of microalgae, use of the inexpensive carbon substrates such as industrial wastes and mixed culture of microalgae. Of these techniques, the mixed culture of microalgae is a convenient solution for achieving the goals. Mixed cultures of microalgae are common in natural ecological systems. They are often used for the treatment of agro-industrial wastes, as well as for the production of biomass and bioactive compounds [2]. Polyculture enhances mixed secondary metabolite production, control the relative proportion of the cells and reduce contamination. Polyculture of microalgae improves the possibility of controlling the production of some bioactive compounds by manipulating the cultivation conditions (molecular farming) [3]. Microalgae adapt rapidly to new environmental conditions to survive, producing a great variety of secondary (biologically active) metabolites [4]. Microalgae content of secondary metabolites can be influenced by the growing parameters (water temperature, salinity, light and nutrients) [5].

Integrating aquaculture production and processing of microalgae would stimulate the development of a sustainable aquaculture industry by providing technology that allows increased aquaculture production while reducing or eliminating the environmental impact of

aquaculture, and simultaneously increasing the profitability of such operations can serve a number of important applications, namely,

- i. to add value to the aquaculture industry
- ii. the discovery of novel compounds will aid the development of new natural product from microalgae and as well serve to give local data on microalgae secondary metabolites in Nigeria that can be used as standards by Institutions charged with natural product research; a major component of the Nigerian agriculture policy
- iii. establishment of the percent crude protein will provide information on the nutritional qualities of microalgae as regards aquaculture feeds
- iv. indicated zone of inhibition exhibited by extracts and isolated compounds on test microorganisms can encourage the development of pharmaceuticals from microalgae
- v. establishment of the fatty acids composition of the oil fraction will aid in evaluating its suitability to replacing fish meal in aquaculture feed making
- vi. establishment of the structures of the isolated compounds will supplement databanks used for designing new organic structures.

This research is focused in identifying bioactive compounds in microalgae in the study area in order to identify appropriate use of the microalgae biomass. This is to encourage the development of aquaculture through specific improvements and innovations (discovery of new sources of existing compounds that might have a wide range of applications as well as finding ways in which existing waste-streams from aquaculture operations might yield useful compounds thus improving the profitability of overall enterprises that might have value for aquaculture industries).

## II. Experimental Methods

### II.1 Collection of microalgae Samples

The microalgae samples was collected from a fish pond. The collection point from concrete fish ponds of National Institute for Freshwater Fisheries Research, New Bussa, Niger State, Nigeria. The Algal mats were washed properly to remove muds and then suspended in liquid medium. The microalgae was identified up to species to know the diversity and abundance, and counted using Sedgewick Rafter Counting Chamber [6] under an inverted divert microscope following the key of [7,8].

### II.2. Isolation of microalgae

Density Centrifugation: The collected samples contained lots of suspended abiotic contaminants, bacteria and a large amount of diverse microorganisms. Repeated low-speed centrifugation (500 - 1000 rpm) removed up to 90 % of the suspended materials and unicellular microorganisms. Microalgae species were found at the upper phase in the floating mass.

Micromanipulation: Algal filaments were picked by the use of a glass micropipette into one drop of medium on a microscope slide and was examined under microscope from time to time to select the pure culture and discard contaminants

### II.3. Identification of microalgae

The first species of *Spirulina* was identified according to [9, 10]. After observation under the microscope at different magnifications and according to the taxonomic guide, the green microalgae species of were identified by observing the trichomes width, cell length, pointed

calyptras, type of coil and helix- shape [11]. The others were identified according to the guideline published in the references of [12, 13, 14, 15 and 16].

#### **II.4. Organic extracts of microalgae**

Organic extracts were made from the pulverized dried samples of microalgae. The organic extraction was performed with predistilled petroleum ether, chloroform, ethyl acetate and methanol. Powdered samples of dried algae were macerated for two weeks in 500 cm<sup>3</sup> of the respective extracting solvents based on increasing polarity in a round bottom flask. After filtration and evaporation using rotary evaporator, the crude extracts were obtained.

#### **II.5. Aqueous extracts of microalgae**

The method of [17] was used for the aqueous extraction. The algal samples were washed and extracted with boiling water for 2 h. After centrifugation at 5000 rpm for 20 mins, the supernatant was concentrated under vacuum at 40°C and precipitated with ethanol to obtain the high molecular weight polysaccharide fraction. The precipitate was dried to yield a brownish powdery crude extract.

#### **II.6. Isolation**

##### **II.6.1. Column chromatography**

Column chromatography, applied on a column of 4 cm external diameter and 35 cm length, was used to isolate the compounds based on their polarity with the respective solvent systems. After coming up with the solvent mixture, the column was packed very tightly in order to achieve uniform separation as the compound moves down the column. The glass column was plugged with cotton wool directly above the stopcock to prevent the silica gel from escaping the column through the stopcock. The different fractions were collected from the column chromatography.

##### **II.6.2. Packing Column Chromatography**

Silica gel 60 (0.06-0.2 mm, 70-230 mesh) was used as stationary phase. Silica gel (40 g) was used for packing the column. The stationary phase was suspended in the less polar solvent (petroleum ether) and stirred gently until slurry suspensions were formed. The suspension was then poured carefully and slowly into the column with tapping on the walls of the column gently with a cushioned rod to encourage any air bubbles to rise to the top of the column. Solvent level was monitored to avoid drying.

##### **II.6.3. Introduction of Sample to Open Column**

The sample was introduced as powder to the top of the column. After the sample was loaded, a small layer of glass wool was added to the top of the column. This helped to keep the top of the column undisturbed when adding solvent for elution.

##### **II.6.4. Isolation of Compounds**

The mobile phase passed through the column under gravity. Hexane fraction was subjected to column chromatography separation in order to isolate the compounds responsible for the observed biological activities. First the elution was done with Hexane-DCM-MeOH (25:63:12) to yield isolate **A**. This was further purified with methanol. The extract was subsequently eluted with warm water (100 %) to give isolate **I** which was also further purified with methanol. Ethyl

acetate fraction was subjected to gravity-driven column chromatography. From the chromatographic column, two isolates **E**: DCM-Acetic acid-MeOH (60:30:10) and **G**: MeOH-H<sub>2</sub>O (3:1) were isolated after further purification processes respectively. The isolates were purified with methanol (100%).

The 20% acetic acid extract was applied to a gravity-driven column chromatography and eluted with warm water (100%). Further purification using n-hexane-EtOAc (1:1) as the eluting solution to give isolate **H**.

Methanol fraction was washed with petroleum ether to remove the lipid components. Then the column was eluted with MeOH-EtOAc (80:20) and MeOH-CHCl<sub>3</sub> (80:20) yielding isolates **B** and **D** respectively. Further purification was done using n-hexane-EtOAc (1:1) on the isolates respectively.

The aqueous extract was loaded onto column packed with silica gel 60 particle size 0.06-0.2 mm (70-230 mesh) (Fluka Chemika) and the column was eluted with H<sub>2</sub>O (100%). Further purification with hexane: ethyl acetate (1:9) produce isolate **O**.

Raw powdered algal material was washed with petroleum ether to remove the lipid components. Then the column was eluted with warm water (100%) yielding isolates **N**. Further purification was done using n-hexane-EtOAc (1:9) on the isolate.

## II.7. Structure Elucidation of Isolated Compounds

### II.7.1. Algal oil Extraction

Algal oil was the first product to be eluted from the isolation processes. The lipid samples were saponified over-night with ethanolic KOH (20%) at room temperature. The fatty acids were freed from their potassium salts by acidification with hydrochloric acid (5%), followed by extraction with petroleum ether (40-60°C). The ether extract was washed three times with distilled water and then dried over anhydrous sodium sulphate and filtered off. Saponified oil was methylated by reacting saponified fraction with 4% H<sub>2</sub>SO<sub>4</sub> in methanol for 24 h at room temperature. The sample was dried and labeled EO. The fatty acids profiles were determined in a GCMS-QP2010 Plus, Shimadzu, Japan gas Chromatograph coupled to a mass selective detector. Separation was carried out in a capillary column (30 x 0.25mm id x 0.25µm DB wax). The starting temperature was 250°C maintained for 2 minutes at a heating rate of 10°C/minutes. The total running time was 22 minutes. Helium was the carrier gas while the injection volume was 1µL. The constituent fatty acids peaks were identified based on retention time, molecular ion peak and characteristic fragmentation pattern in the mass spectrum. These are then compared with the retention time and molecular mass of mass spectra of standard, obtained from library (Wiley and NIST) of the instrument.

### II.7.2. Nuclear Magnetic Resonance Spectroscopy (NMR)

Solid-state cross polarisation (CP) and magnetic angle spinning (MAS) <sup>13</sup>C-NMR spectra were carried out on a 363 MHz Tecmeg spectrometer in the Centre for Solid-State NMR Spectroscopy of the Spectral Data Services Inc, 818 Pioneer Champaign, IL61820, USA. The polarisation of <sup>1</sup>H and <sup>13</sup>C were done at frequencies of 363.331 and 91.3695 MHz at room temperature respectively. The Hartmann-Hahn condition (effective CP transfer and reduced spinning side bands exhibition) to minimize overlapping between the main signals (aliphatic and aromatic carbon) and the spinning side bands (SSB) was achieved with the radio frequency field

strength of 14.9 kHz, a typical cross-polarisation times of 1  $\mu$ s, acquisition times of 5  $\mu$ s, and recycle delays of 3s for fresh samples. Sample (200 mg) were packed into a 7 mm zirconia rotor with a Kel-F cap and spun at the magnetic angle of 54°74' with respect to the magnetic field. This is to make chemical shift anisotropy and dipolar couplings that are less than the spinning speed averaged to zero at a rate of 7 kHz. In order to circumvent spin modulation of Hartmann-Hahn conditions, a single contact spin-lock cross-polarisation sequence was used with a pulse to flip back the remaining  $^1\text{H}$  magnetisation after acquisition. A 90-degree pulse of 5  $\mu$ s and a recycle delay of 3 s were used [17]. The spectra were obtained at room temperature averaging over 1008–12000 scans.

Chemical shifts are reported relative to tetramethylsilane (TMS) at 0 ppm. (NMR chemical shifts are measured in parts per million of frequency from a reference. For  $^{13}\text{C}$  at 2.35 T, 1 ppm corresponds to a shift of 25.18 Hz from TMS). Because the spectra were run at low field (2.35 T), there was no distortion of intensity due to generation of satellite lines known as spinning side bands. All the spectra were divided in the following regions whose assignment is fully discussed later: 0-40 (alkyl C), 40-60 (O/N alkyl C), 96–110 (O–C–O anomeric) and 160-180 (COOH groups) ppm. In order to separate the signals of  $\text{sp}^3$ -hybridised anomeric C (O–C–O) from those of  $\text{sp}^2$ -hybridised aromatic C, both of which may resonate between 120 and 90 ppm, the aromatic-C signals were selectively suppressed by a five-pulse  $^{13}\text{C}$  chemical-shift anisotropy (CSA) filter with a CSA-filter time of 5  $\mu$ s. In particular, this technique identifies anomeric O–C–O C, around 100 ppm typical of sugar rings [18].

### III. Results

#### III.1. Microalgae Species Identification

The microalgae species (8 green, 4 yellow and 4 blue-green) identified in the sample are presented in Table 1. The percent composition of the species were *Chlorella ellipsoidea* (55%), *Diatomella* species (11%) and *Aphanacapsa* species (26%) of the microalgae are presented in Figure 1.

Table 1: Microalgae species identified in study area

Green algae	Yellow-green algae	Blue-green algae
<i>Scenedesmus quadricanda</i>	<i>Fragillaria species</i>	<i>Aphario capsaeladista</i>
<i>Scenedesmus incrassatulus</i>	<i>Diatomella species</i>	<i>Microcystis species</i>
<i>Staurastrum rotula</i>	<i>Navicula digitoradiata</i>	<i>Athrospira species</i>
<i>Chlorella ellipsoidea</i>	<i>Nitzschia dissipata</i>	<i>Aphanacapsa species</i>
<i>Pediastrum simplex</i>		
<i>Hormidium species</i>		
<i>Closterium species</i>		
<i>Akistrodesmus species</i>		

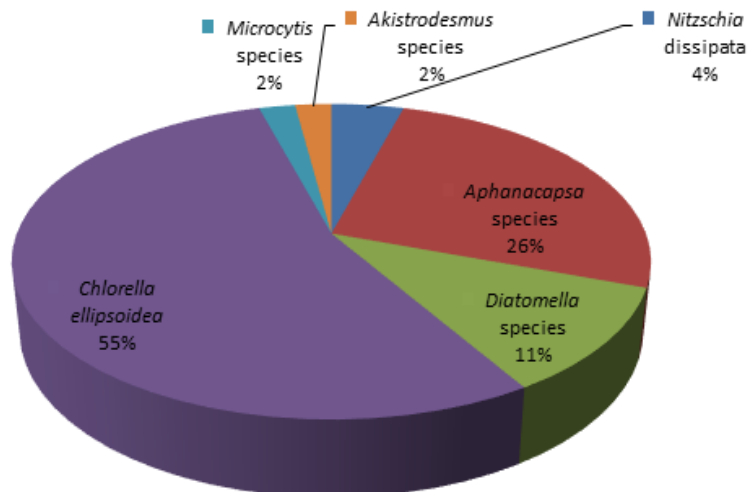


Figure 1: Percent species of microalgae identified in study sample

### III.2. Identification and Determination of Fatty Acids by GC-MS

The total ion chromatogram (Figure 2) of the lipid fraction, retention time (RT), molecular formula, molecular weight (MW) and concentration (%) are presented in Table 2. Thirteen fatty acids, which is made up of three monounsaturated fatty acids (34.38%), three polyunsaturated fatty acids (16.79%) as well as seven saturated fatty acids (47.48%) are presented in Table 2.

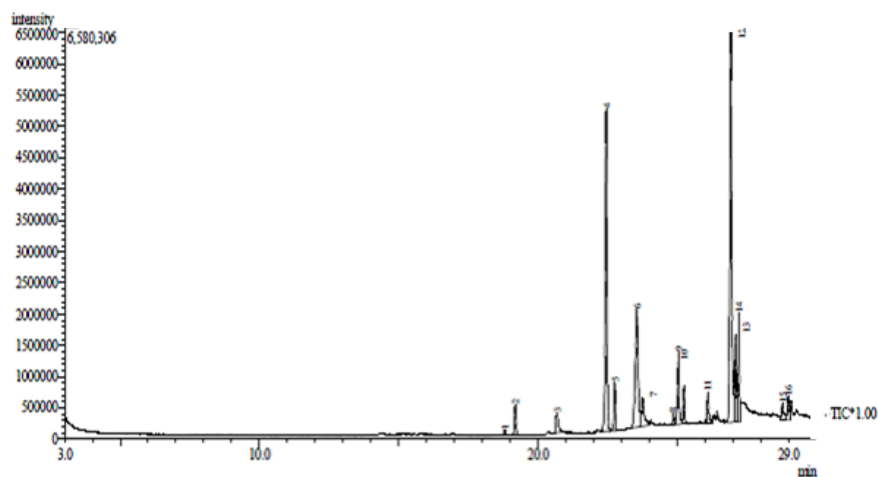


Figure 2: total ion chromatogram (TIC) of oil fraction

Table 2: Fatty acids identified in algal oil

Peak	R. Time	Area %	Base peak	Molecular ion	Molecular Formula	Name
1	18.814	0.32	55	98	C <sub>5</sub> H <sub>6</sub> O <sub>2</sub>	Methyl-2,3-butdienoate
2	19.195	1.95	74	270	C <sub>17</sub> H <sub>34</sub> O <sub>2</sub>	Methyl-n-hexadecanoate
3	20.688	1.87	43	256	C <sub>16</sub> H <sub>32</sub> O <sub>2</sub>	Methyl-n-pentadecanoate
4	22.463	21.70	55	296	C <sub>19</sub> H <sub>36</sub> O <sub>2</sub>	Methyl-9-octadecenoate
5	22.764	2.40	74	298	C <sub>19</sub> H <sub>38</sub> O <sub>2</sub>	Methyl-n-octadecenoate
6	23.561	14.34	55	264	C <sub>17</sub> H <sub>28</sub> O <sub>2</sub>	Methyl-3,5,7-hexadectrienoate
7	23.767	3.17	43	284	C <sub>18</sub> H <sub>36</sub> O <sub>2</sub>	Methyl-n-heptadecanoate
8	24.863	0.60	55	129	C <sub>7</sub> H <sub>13</sub> O <sub>2</sub>	Methyl-3-hexenoate
9	25.056	4.77	43	268	C <sub>17</sub> H <sub>32</sub> O <sub>2</sub>	Methyl-3-hexadecenoate
10	25.258	1.92	74	326	C <sub>21</sub> H <sub>42</sub> O <sub>2</sub>	Methyl-n-eicosanoate
11	26.110	2.13	59	126	C <sub>7</sub> H <sub>10</sub> O <sub>2</sub>	Methyl-3,5-hexdienoate
12	26.938	30.25	55	338	C <sub>22</sub> H <sub>42</sub> O <sub>2</sub>	Methyl-uncosanoate
13	27.098	5.52	43	296	C <sub>19</sub> H <sub>36</sub> O <sub>2</sub>	Methyl-9-octadecenoate
14	27.224	5.92	74	354	C <sub>23</sub> H <sub>46</sub> O <sub>2</sub>	Methyl-n-docosanoate
15	28.794	1.48	55	129	C <sub>7</sub> H <sub>13</sub> O <sub>2</sub>	Methyl-3-hexenoate
16	29.003	1.66	43	129	C <sub>7</sub> H <sub>13</sub> O <sub>2</sub>	Methyl-3-hexenoate

### III.3. Spectral Data for the Isolated Compounds

The <sup>13</sup>C-NMR spectra of the isolated compounds obtained from a 363 MHz, Tecmag (USA) Spectrometre Instrument at a field strength corresponding to 91.3695 MHz for <sup>1</sup>H and 363.331 MHz for <sup>13</sup>C at ambient temperature are presented in figures 4.12 - 4.20. The spectra are divided into: 0-40 (alkyl C), 40-60 (O/N alkyl C), 96-110 (O-C-O anomeric) and 160-180 (COOH groups) ppm.



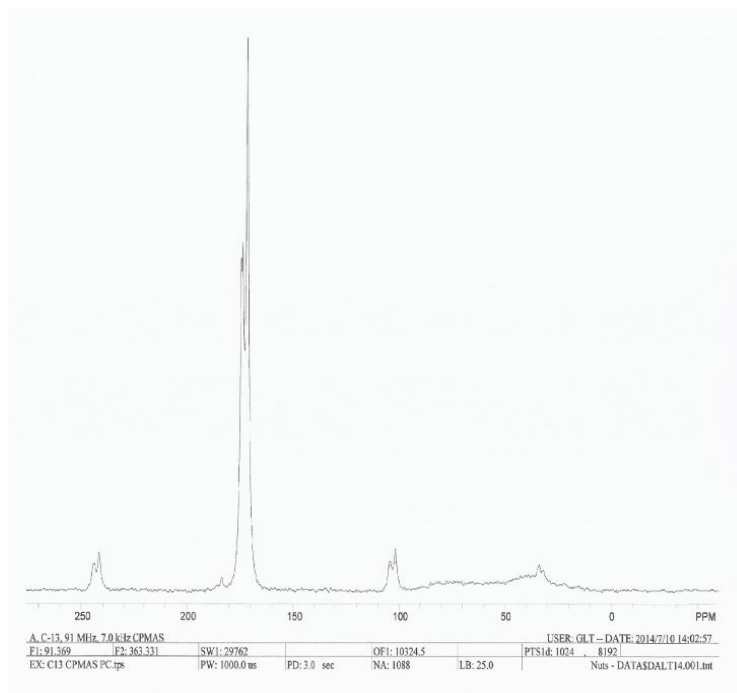


Figure 3: <sup>13</sup>C NMR Spectrum for Glycylglycylglycylglycine (A) at 91.369 MHz with reference to TMS at 0 ppm. The signal at  $\delta$ 33.6 ppm indicated methylene carbon while signals  $\delta$ 174-171 ppm are amide group carbons of glycine units.

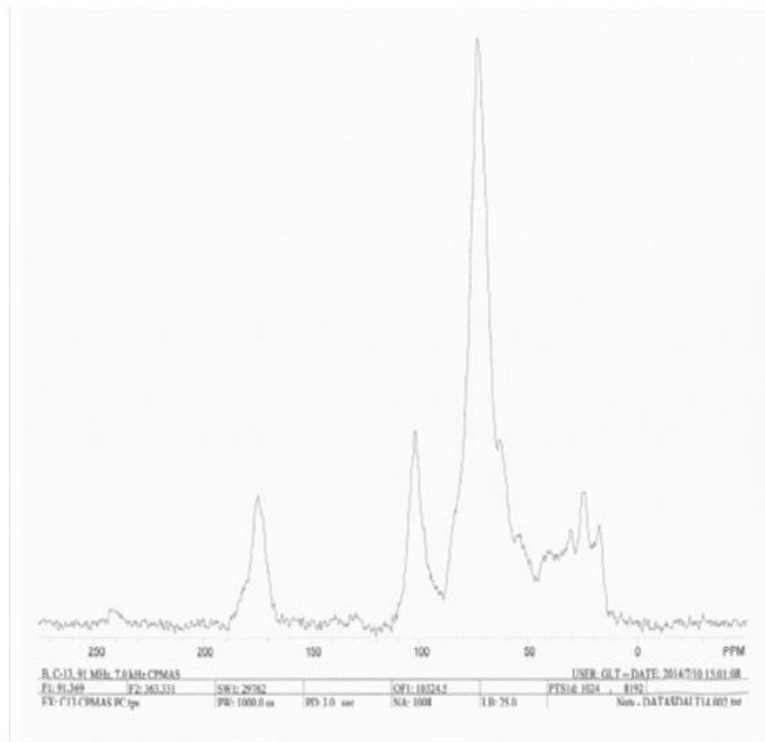


Figure 4: <sup>13</sup>C NMR Spectrum for  $\alpha$ -D-mannopyranosyl-2-amino-3-methylbutanoic acid (B) at 91.369 MHz with reference to TMS at 0 ppm. Peaks at  $\delta$ 24.8-17.3 ppm are methyl carbon atoms,  $\delta$ 102.2 ppm is the anomeric carbon atom of and  $\delta$ 174.5 ppm indicates a carboxylic carbon of valine unit.

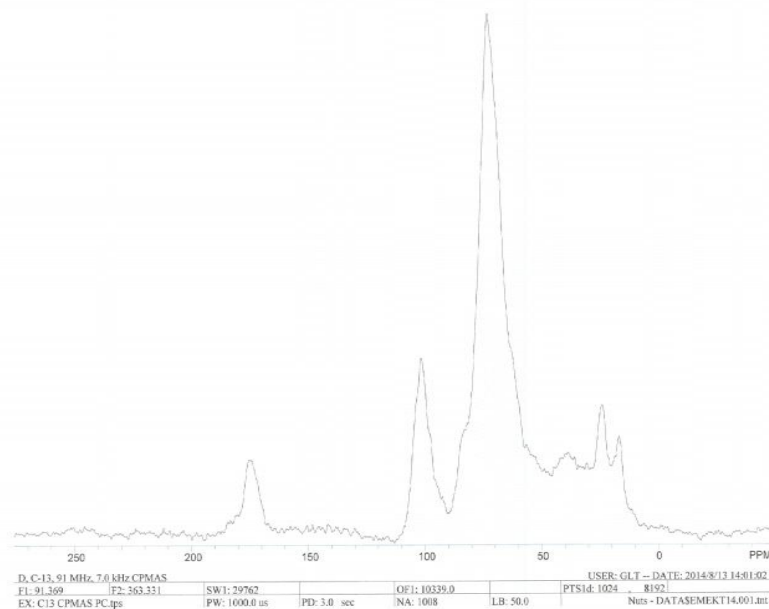


Figure 5:  $^{13}\text{C}$  NMR Spectrum for  $\alpha$ -D-mannopyranosyl-3-aminobutanoic acid (D) at 91.369 MHz with reference to TMS at 0 ppm. The peaks at  $\delta$ 38.7-16.9 ppm are for saturated alkyl carbons of the aliphatic amino acid ( $\beta$ -alanine),  $\delta$ 101.7 ppm is the anomeric carbon while the carbonyl carbon in the peptide bond is  $\delta$ 174,7 ppm.

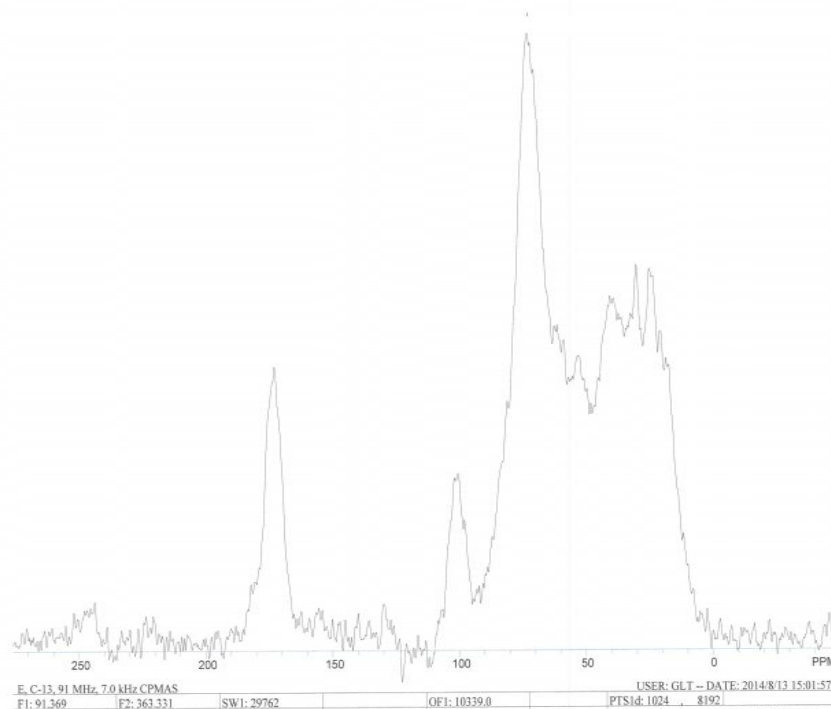


Figure 6:  $^{13}\text{C}$  NMR Spectrum for  $\alpha$ -D-glucopyranosyl-2-aminomethyl-4-methylpentanoic acid (E) at 91.369 MHz with reference to TMS at 0 ppm. The methyl carbon atoms peaks occur at  $\delta$ 20.8-17.4 ppm, the methylene carbon atoms at  $\delta$ 30.2-25.0 ppm,  $\delta$ 58.8 ppm is an O-alkyl carbon atom while the peak at  $\delta$ 173.0 ppm is the carbonyl carbon of the leucine residue.

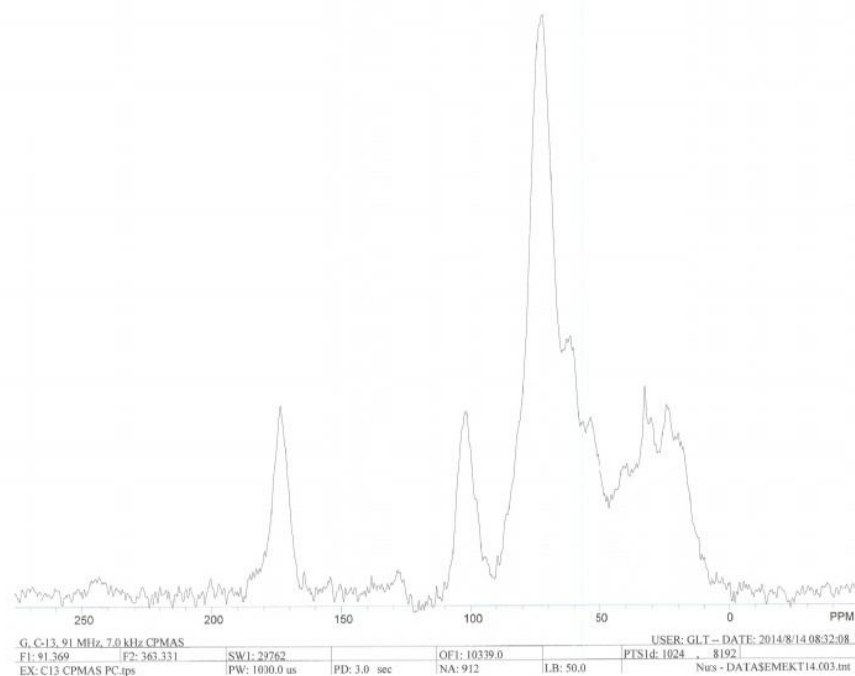


Figure 7:  $^{13}\text{C}$  NMR Spectrum for  $\alpha$ -D-glucopyranosyl-2-amino-4-methylmethylpentanoate acid (G) at 91.369 MHz with reference to TMS at 0 ppm. The peaks at  $\delta$ 23.5-17.9 ppm is the methyl carbon atoms of the leucine residue, a methane carbon atom is  $\delta$ 40.4 ppm. The signals  $\delta$ 62.8 and  $\delta$ 71.8 ppm indicate C-6 and C-2,3,5 respectively.

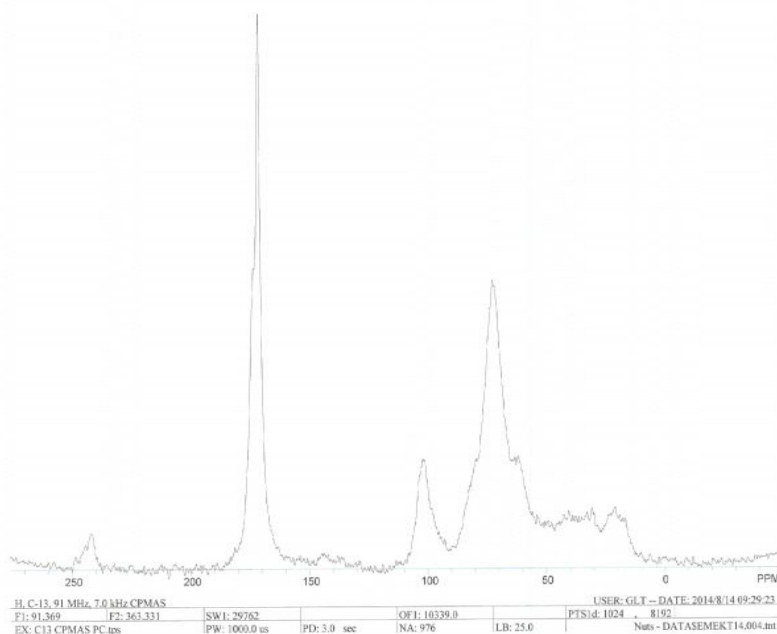


Figure 8: Figure 4.14:  $^{13}\text{C}$  NMR Spectrum for  $\alpha$ -D-glucopyranosyl-glycylglycine (H) at 91.369 MHz with reference to TMS at 0 ppm. The resonances at  $\delta$ 20.9 and 30.7 ppm indicated secondary methyne carbon atoms of the glycine dipeptide,  $\delta$ 102 ppm is the anomeric carbon atom while  $\delta$ 171.4 and  $\delta$ 173.4 ppm indicated the carbonyl carbon atoms in the peptide bonds.

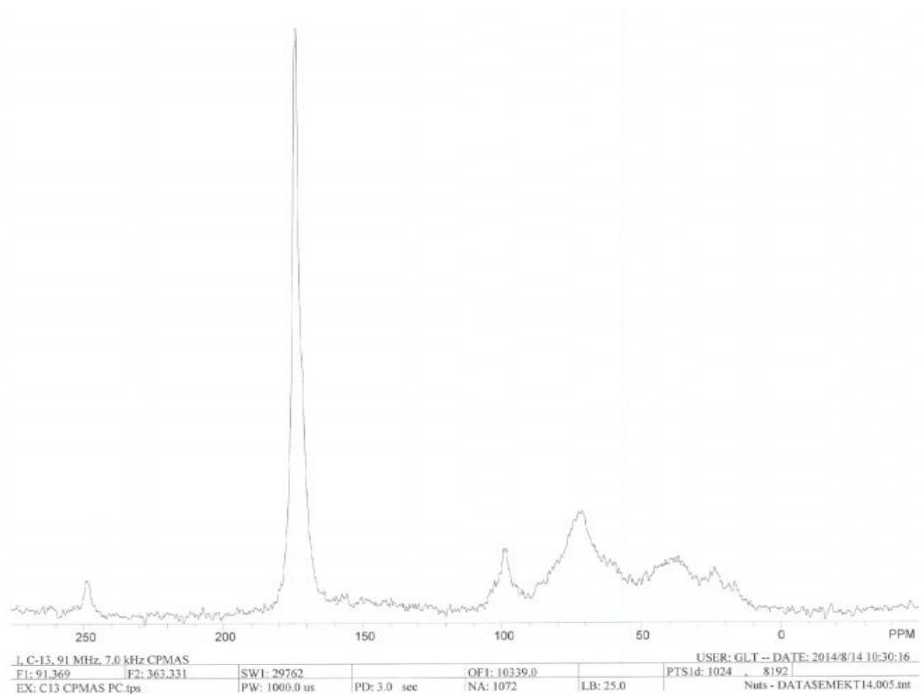


Figure 9:  $^{13}\text{C}$  NMR Spectrum for  $\alpha$ -D-glucopyranosyl-3-aminobutanoic acid (I) at 91.369 MHz with reference to TMS at 0 ppm. Peaks at  $\delta$ 23.7 and 16.5 ppm are the methylene carbon atoms of the  $\beta$ -alanine residue,  $\delta$ 71.1 ppm indicated C-2,3,5 while  $\delta$ 174.1 ppm is a carbonyl carbon in the peptide bond.

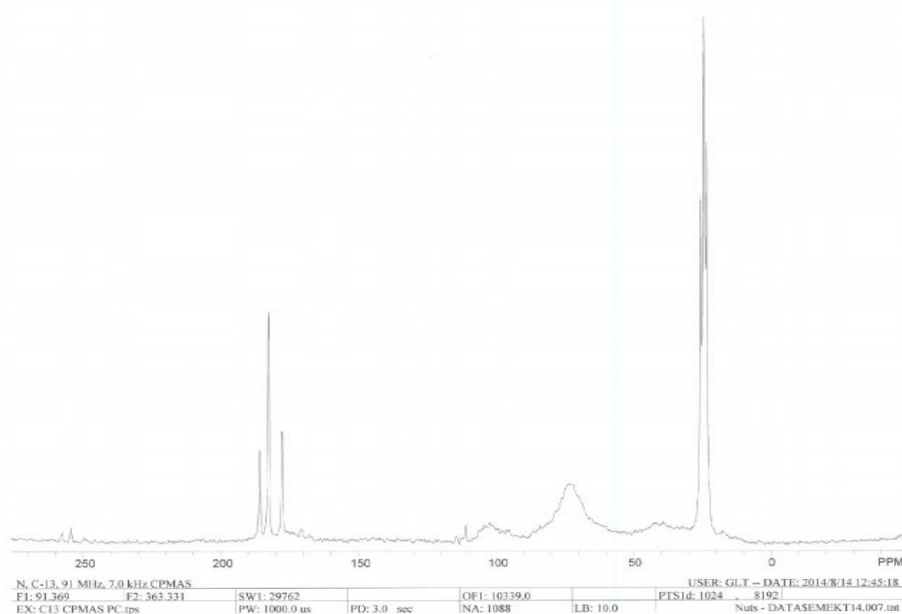


Figure 10:  $^{13}\text{C}$  NMR Spectrum for  $\alpha$ -D-glucopyranosyl-2, 4, 6-triamino-4-methylheptanoic acid (N) at 91.369 MHz with reference to TMS at 0 ppm. The peak at  $\delta$ 102.3 ppm corresponds to C-1 carbon atom in the  $\alpha$ -glycosidic bond, while the signals at  $\delta$ 177.7, 182.6 and 185.8 ppm are located in the carbonyl region and can be assigned to two amide group carbons and a carboxylic carbon respectively. The chemical shifts of  $\delta$ 71.9 ppm correspond to those of carbons 2, 3, 5 respectively of  $\alpha$ -glucopyranose residues.

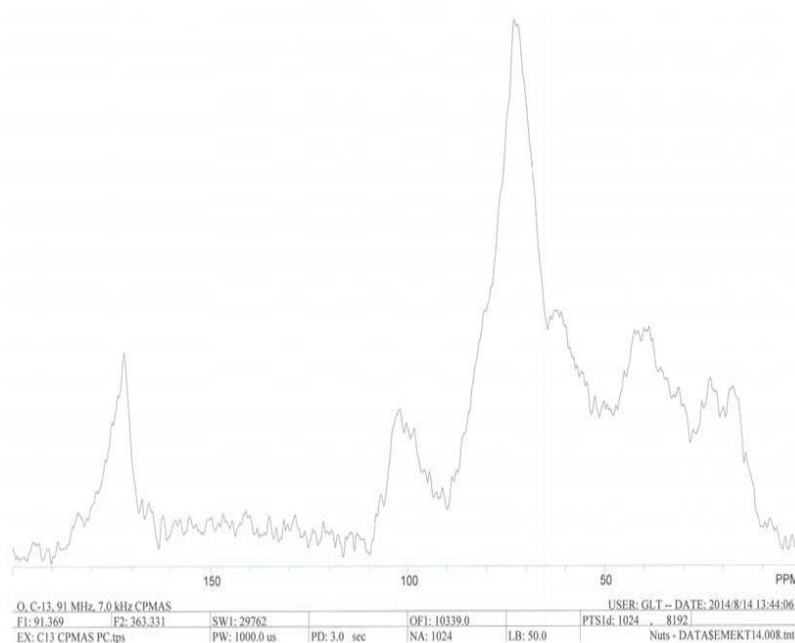


Figure 11:  $^{13}\text{C}$  NMR Spectrum for  $\alpha$ -D-glucopyranosyl-2-amino-3-methylpentanoic acid (O) at 91.369 MHz with reference to TMS at 0 ppm. The aliphatic alkyl chain carbons;  $\delta$ 17.5 ( $\text{CH}_3$ ) ppm,  $\delta$ 23.2 ( $\text{CH}_2$ ) ppm,  $\text{C}\beta$  signal is  $\delta$ 38.8 (CH) while  $\text{C}\alpha$  42.5(CH) bonded to  $\text{NH}_2$  will resonate at 41.2 ppm. The peak at  $\delta$ 171.7 ppm is the carbonyl carbon ( $\text{C}=\text{O}$ ). The chemical shifts of  $\delta$ 62.8, 71.8 ppm correspond to those of carbons 6, 2, 3, 5 respectively of  $\alpha$ -glucopyranose residues.

Table 3:  $^{13}\text{C}$  resonance assignments of the CP/MAS solid-state NMR spectra from Figures A-N

A	B	D	E	G	H	I	O	N	Assignment
	17.3		17.4	17.9			17.5		$\text{CH}_3$ [19]
	24.8		20.8	23.5					$\text{CH}_3$ [20]
33.6		16.9	25.0			16.5		23.5	$\text{CH}_2$ [21]
		24.1	30.2	30.2		23.7	23.2	24.5	$\text{CH}_2$ [19]
								25.6	$\text{CH}_2$ [19]
	41.2	38.7	40.6	40.4	20.9		38.6	39.3	CH [22]
					30.7	39.4	42.5	41.4	CH [22]
	30.8			32.5					$\text{CR}_4$ [19]
			50.8						N-alkyl carbon [23, 24]
			58.8	53.6					O- $\text{CH}_3$ [23, 25, 26]
	63.1		62.5	62.8	61.8		62.8		C6 [27]
	73.4	73.2	72.9	71.8	72.6	71.1	71.8	71.9	C2, 3, 5 [28]
					79.6				C-4 [29]
	102.2	101.7	100.5	101.8	102.0			102.3	C-1 [25, 26, 29, 30, 31]
171.6					171.4		171.7	177.7	C=O [32]
173.8			173.0	173.2	173.4				C=O [33]
174.5	174.5	174.7				174.1		182.6	C=O [34]
183.5								185.8	COOH [20]

## IV. Discussion

### IV.1. Microalgae Source

Table 1 showed the various species of microalgae that were detected in fish ponds during the study while Figure 1 indicated the microalgae detected in the sample material. It seems that though microalgae can be harvested from the wild by harvesting natural blooms, however may contain different microalgae strains. Therefore open ponds are highly unpredictable and uncertain source of biomass due to the inherent contamination with other species of microalgae. The sample biomass contained about 55% *Chlorella ellipsoidea*, *Aphanacapsa species* (26%), *Diatomella species* (11%), *Nitzschia dissipata* (4%) while *Microcystis species* and *Akistrodesmus species* (2%). *Chlorella ellipsoidea* are adaptable to nutrient-rich media [35]. The source concrete fish pond was used for fish farming. The existence of favourable climatic conditions and sufficient nutrients encourages the growth of microalgae. In order to avoid contamination, rather extreme cultivation conditions should be chosen (i.e. high salinity, high pH, and high nutrients concentration to ensure the existence of a monoculture [36].

### IV.2. Characterisation of Fatty Acids from Microalgae Oil

Typically, characterisation of microalgae lipids involves breaking down the triglycerides and other intact lipids, followed by the derivation of fatty acids to fatty acid methyl esters prior to analysis by GCMS.

GC-MS analysis of the microalgae oil revealed many known fatty acids (Figure 2). Their constitution and structure were established based on retention time, molecular ion peak (Table 2) and characteristic fragmentation pattern in the mass spectrum. These straight chain aliphatic compounds showed a series of peaks at  $m/z = 15 + 14n$ , where  $n$  is the number of  $\text{CH}_2$  groups in the chain and  $m/z = 15$  corresponds to the terminal methyl group. Fatty acids with general formulae of  $\text{CH}_3(\text{CH}_2)_n\text{CO}_2\text{H}$  have a long linear hydrocarbon chain. They undergo a typical fragmentation pattern which is used to obtain structural information.

Generally, the mass spectra of the methyl esters were composed of  $\text{CH}_3(\text{CH}_2)_n^+$  ( $m/z 15+14n$ ) and  $[(\text{CH}_2)_n\text{CO}_2\text{H}]^+$  ion distributions; hydrocarbon peaks and oxygen-containing peaks respectively. The hydrocarbon peaks are due to positive charge retention by the hydrocarbon end of the molecule. The oxygen-containing fragments are due to the cleavage, breaking of a single bond, and those formed by breaking several bonds with rearrangement of atoms to make a fragment not found in the original molecule. Series of simple cleavage peaks found in the mass spectra have the general formula  $\text{CH}_3\text{OOC}(\text{CH}_2)_n$ . There was no particular abundant ion in the mass spectra. This could be as a result of the variation of the fatty acids contained.

The data in Table 2, shows that the microalgae oil is composed of thirteen fatty acids, which is made up of three monounsaturated fatty acids; C6:1 (Hex-3-enoic acid), C16:1 (Hexadec-3-enoic acid) and C18:1 (Octadec-9-enoic acid), three polyunsaturated fatty acids; C4:2 (but-2, 3-dienoic acid), C6:2 (Hex-3, 5-dienoic acid) and C16:3 (Hexadec-3, 5, 7-trienoic acid) as well as seven saturated fatty acids; C15:0 (n-Pentadecanoic acid), C16:0 (Hexadecanoic acid), C17:0 (n-Heptadecanoic acid), C18:0 (n-Octadecanoic acid), C20:0 (n-Eicosanoic acid), C21:0 (n-Uncosanoic acid) and C22:0 (n-Docosanoic acid) were identified. The saturated fatty acids are the major components in the microalgae lipids (47.48% of the total). The monounsaturated fatty acids are 34.38% while the polyunsaturated fatty acids are 16.79%. The percent of  $\omega$ -3 fatty acids detected is 19.11%. Among the saturated fatty acids, C16:0 (palmitic acid) is the major portion, which is similar to many other vegetable oils, such as soybean oil. In a typical soybean oil, 6% to 8% of the lipids are palmitic acid (C16:0), 2% to 5% are stearic acid (C18:0), 20% to

30% are oleic acid (C18:1), 50% to 60% are linoleic acid (C18:2), and 5% to 11% are linolenic acid (C18:3) [37]. These lipids were found in the microalgae oils in relatively similar proportions. This finding indicates that microalgae oils are good candidates for biodiesel production because their fatty acid profiles are similar to that of soybean oil, which is currently the primary resource of biodiesel production in the U.S. The fatty acid profiles obtained from the selected microalgae oils in this study are also in agreement with those published for various strains by other researchers. The tested microalgae oils all contain C16:0 and C18:1 fatty acids, which are the major constituents of their fatty acid profiles [38, 39].

The ability of cells to accumulate PUFAs is intrinsically limited in most algae, since these fatty acids are generally components of membrane lipids whose content is strictly regulated. A number of studies have found bioactivity in the free fatty acid fraction of algal lipids. [40, 41] observed that PUFA exhibited antimicrobial activity against a wide range of microorganisms. Therefore it could be inferred that the PUFA were partly responsible for the bioactivities observed in this study.

### IV.3. Structure Elucidation by Solid-State $^{13}\text{C}$ Nuclear Magnetic Resonance

The bioactivity data from the screening of antioxidant and antibacterial activities were the background for evaluating isolates for structure elucidation. In order to narrow down the search for the active constituents of the extracts, and because the algal biomass contains some lipids (Figure 2), the first challenge consisted in separating these lipids from the other compounds of interest. For this purpose, preliminary washing of the extracts with methanol-dichloromethane as mobile phase, enabled an appropriate isolation.

In order to get first structural information, the isolates were subjected to analysis by solid-state  $^{13}\text{C}$  NMR. There were no useful data obtained from solution state NMR,  $^1\text{H}$  NMR and GC-MS as all the isolates were insoluble in common laboratory solvents. Therefore, the  $^{13}\text{C}$  NMR spectra were recorded in the broad band decoupled mode in order to avoid the extensive signal overlap which can occur due to the large one bond carbon hydrogen coupling constants (ca. 120-250 Hz). The multiplets are thus reduced to single lines and it is possible to determine the number of carbons. Usually, the carbon resonances representing the carbohydrate rings (furanose or pyranose form) are not superimposed and give rise to independent signals.

Therefore the number of anomeric carbons can be readily determined by  $^{13}\text{C}$  NMR, defining the number of individual sugar residues present. However, the six ring carbons can give rise to fewer than six signals when the ring is unsubstituted or possesses symmetrical substitution [42].

In this study, the carbon signals assignments had taken the following into consideration:

- i. The spectrum of liquid state and solid state NMR are distinct. The liquid state spectra are characterised by sharp narrow lines while solid state spectra are broad.
- ii. The cross-polarisation magnetic-angle spinning (CPMAS) method uses a combination of techniques to over-come the problems of broadening and low signal intensity for  $^{13}\text{C}$  NMR of solids [43]. Line narrowing is achieved with high-power decoupling to remove  $^{13}\text{C}$ - $^1\text{H}$  dipolar interactions, plus magnetic-angle spinning to eliminate broadening due to chemical shift anisotropy. (In the latter, the sample is rotated at several kilohertz at an angle of  $54.7^\circ$  with respect to the magnetic field.) Signal intensity increased by cross-polarisation, in which magnetisation is transferred to the  $^{13}\text{C}$  spin population from the more abundant, faster relaxing, and more highly polarisable spins.
- iii. Carbon resonances representing the carbohydrate rings (furanose or pyranose) are not superimposed but give rise to independent signals. However, the ring carbons can give

- rise to fewer signals when the ring is unsubstituted or possesses symmetrical substitution [42].
- iv. The number of anomeric carbon signals defines the number and configuration of individual sugar residues present in the compound [44, 45].
  - v. Pyranose takes chair conformations as long as there is no stereo-electronic interference among the substituent and resonate at 90-110 ppm [45].
  - vi. The C-4 carbon peak appears over a wide range (90-80 ppm) due to the intramolecular hydrogen bonds between the C-3 hydroxyl and O<sub>5</sub> ring oxygen [46].
  - vii. The C-2, C-3 and C-5 resonances overlap with each other in the range 77-73 ppm and therefore may not be assigned individually [46].
  - viii. Alpha-D-glucopyranose exist in two possible conformers; 'a', in which C-4 is situated above, and C-1 below, the plane consisting of C-2, C-3, C-5, and O, and 'b' in which the relationships are the opposite. However, 'a' is naturally more stable but depending on the type of carbohydrate, 'b' and a state of rapid inversion between 'a' and 'b' sometimes exist. This could be the reason why in all the spectra obtained, C-2, 3, 5 as well as C-1 and C-4 appeared as single peaks. Discrepancies in <sup>13</sup>C shifts have not been found between polysaccharides of identical conformation. Since <sup>13</sup>C shifts are primarily determined by the electron state in the vicinity of the <sup>13</sup>C nucleus, such conformation dependence should naturally be expected. Therefore, it is certain that conformation dependence of <sup>13</sup>C shifts exists in carbohydrates if no rapid intramolecular rotations occur [47].
  - ix. The polarisation rate of <sup>13</sup>C nuclei depends on the magnitude of the dipole-dipole interaction between <sup>13</sup>C and <sup>1</sup>H spins. Therefore polarisation rates increases in the order CH<sub>3</sub> > CH<sub>2</sub> > CH respectively. However, when the carbon is also bond to NH<sub>2</sub>, it resonates at higher chemical shift [48].
  - x. The β, γ and δ-carbons of the aliphatic amino acids signals occur at 20–40 ppm while the α-carbons peaks occur at 40–58 ppm [49, 50].
  - xi. When an amino acid molecule exhibits more than one different conformation, the <sup>13</sup>C signals are split because of the different conformations. The carbonyl signals are accompanied by several signals of the amidic carbons. Compounds of identical conformation do not have differences in their chemical shifts [51].

#### IV.4.Spectral Data Analysis of Isolated Compounds

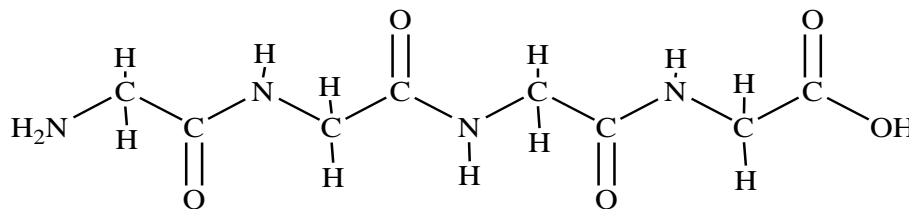
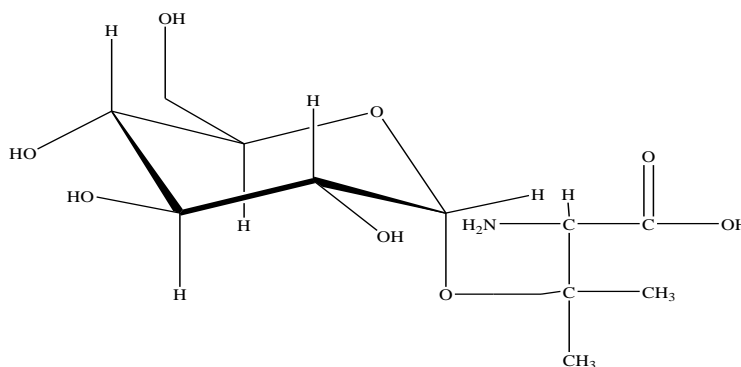
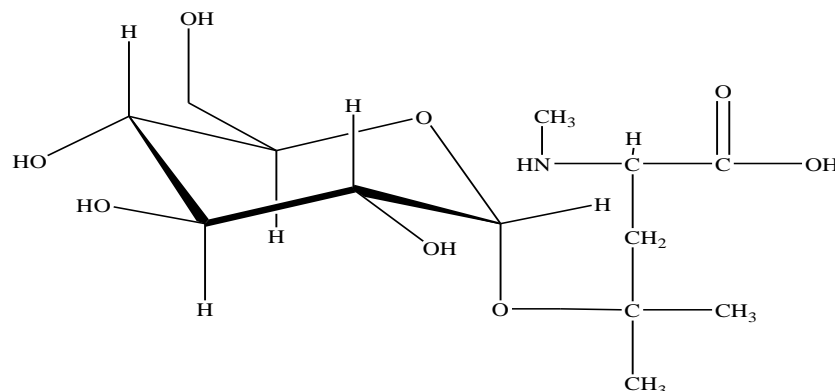
Compound **A** was isolated as an insoluble brownish powder with Hexane-DCM-MeOH (25:63:12) from hexane extract. The <sup>13</sup>C-NMR spectrum (see Figure 3) exhibited 5 signals for 8 carbon atoms from accumulated transient of 1088. These were one methyl carbon at δ33.6 (CH<sub>2</sub>) ppm, three signals at δ171.6, 173.8, 174.5 (amide group carbons) and a carboxylic carbon at δ183.5 ppm. The composed pattern of carbonyl signals (174-171 ppm) proved the existence of numerous polymorphic structures. A sharp peak at 183.5 ppm (carboxylate) is accompanied by three signals of the amidic carbons. The signal at δ33.6 ppm correlates with the methylene group, indicating that the compound contains only one conformer in its unit cell [52]. The CP-MAS <sup>13</sup>C NMR spectrum of glycine consists of two sets of signals; the carboxylic carbon and the methylene carbon [53]. This occurrence of a variety of structures in the solid tetra peptide is probably caused by the existence of conformational liability as well as cis-trans isomerism in amide bonding. Glycine (Amino acetic acid) is the only amino acid with two carbon atoms. The <sup>13</sup>C NMR data obtained for **A** were identical with published data for tripeptide (glycylglycylglycine) [51]. The <sup>13</sup>C NMR data in combination with published data confirmed **A** as a tetra peptide (glycylglycylglycylglycine) with elemental composition as C<sub>8</sub>H<sub>14</sub>N<sub>4</sub>O<sub>5</sub>.



The  $^{13}\text{C}$  NMR spectrum for the insoluble brownish substance (**O**) isolated with  $\text{H}_2\text{O}$  from 10% HCl extract indicated 8 carbon signals (see Figure 11) from accumulated transient of 1024. The aliphatic alkyl chain carbons;  $\delta 17.5$  ( $\text{CH}_3$ ) ppm,  $\delta 23.2$  ( $\text{CH}_2$ ) ppm,  $\text{C}\beta$  signal is  $\delta 38.8$  ( $\text{CH}$ ) while  $\text{C}\alpha$   $42.5$  ( $\text{CH}$ ) bonded to  $\text{NH}_2$  will resonate at 41.2 ppm. The two methyl groups (17.5 and 23.2 ppm) are usually coupled to the same beta carbon. The peak at  $\delta 171.7$  ppm is the carbonyl carbon ( $\text{C}=\text{O}$ ). The amino acid was identified as valine residue (2-amino-3-methylbutanoic acid). The spectrum confirmed the presence of only one sugar moiety with a single anomeric carbon peak at  $\delta 102$  (C-1) ppm. The chemical shifts of  $\delta 62.8$ , 71.8 ppm correspond to those of carbons 6, 2, 3, 5 respectively of  $\alpha$ -glucopyranose residues. The C-6 signals have shoulders between 74-71 ppm. Chemical shifts of  $\delta 73$ -72 ppm are characteristic of  $\alpha$ -D-glucopyranose units. Based on the above results and comparing with published data, **O** were identified as  $\alpha$ -D-glucopyranosyl-2-amino-3-methylbutanoic acid.

This compound (**E**) was eluted with DCM-Acetic acid-MeOH (60:30:10) from a silica gel column from the crude ethyl acetate extract. Upon removal of the solvent mixture under vacuum an impure solid was obtained which was purified with methanol to give an insoluble crystal solid. The  $^{13}\text{C}$  NMR spectrum (Figure 6) indicated signals of  $\delta 17.4$  ( $\text{CH}_3$ ), 20.8 ( $\text{CH}_3$  branched), 25.0 ( $\text{CH}_2$ ), 30.2 ( $\text{CH}_2$ ), 40.6 ( $\text{CH}$ ), 50.8 (N-alkyl carbon), 58.8 (O-alkyl carbon), 62.5 (C-6), 72.9 (C-2, 3, 5), 100.5 (C-1) and 173.0 ( $\text{C}=\text{O}$ ) ppm from accumulated transient of 1056. Due to rapid methyl group rotation, the methyl carbon is assigned 17.4 ppm, the  $\text{C}\sigma$  ( $\text{CH}_2$ ) is 20.8 ppm,  $\text{C}\gamma$  ( $\text{CH}$ ) is 25 ppm,  $\text{C}\beta$  ( $\text{CH}_2$ ) is 30.2 ppm while the  $\text{C}\alpha$  ( $\text{CH}$ ) is 40.6 ppm. The two methyl ( $\delta 17.4$  and 20.8) groups are coupled to the same  $\text{C}\gamma$ . The  $^{13}\text{C}$  signals arising from the  $\text{C}\alpha$  and  $\text{C}\beta$  carbons showed that those assigned to  $\text{C}\alpha$  are wider than those assigned to  $\text{C}\beta$  and both are wider than the remaining aliphatic resonances. This is probably due to the well-known phenomenon of residual dipolar interaction with  $^{14}\text{N}$  due to second order quadrupolar effects. The carbonyl signal peak appears at  $\delta 173$  ( $\text{C}=\text{O}$ ) ppm. The amino acid residue is leucine (2-amino-4-methylpentanoic acid). The second spectral interval between 50 and 60 ppm is traditionally attributed to nitrogenated and oxygenated alkyl systems (Figure 6). Two signals positioned at 50.8 and 58.8 ppm were evidenced in the spectra. That at 50.8 ppm can be assigned to N-alkyl carbons in the carbohydrate segment. The shoulder at 58.8 ppm can be attributed to O-alkyl groups in branched molecules. The  $^{13}\text{C}$  NMR spectrum showed the presence of one anomeric carbon at  $\delta 100.5$  ppm and confirms a single carbohydrate residue. The chemical shifts of  $\delta 62.5$ , 72.9 ppm correspond to those of carbons 6, 2, 3, 5 respectively of  $\alpha$ -glucopyranose residues. The C-6 signals have shoulders between 74-71 ppm. Chemical shifts of  $\delta 73$ -72 ppm are characteristic of  $\alpha$ -D-glucopyranose units. The  $^{13}\text{C}$  NMR data in combination with published data, identified **E** as  $\alpha$ -D-glucopyranosyl-2-aminomethyl-4-methylpentanoic acid with elemental composition as  $\text{C}_{14}\text{H}_{26}\text{N}_2\text{O}_7$ .

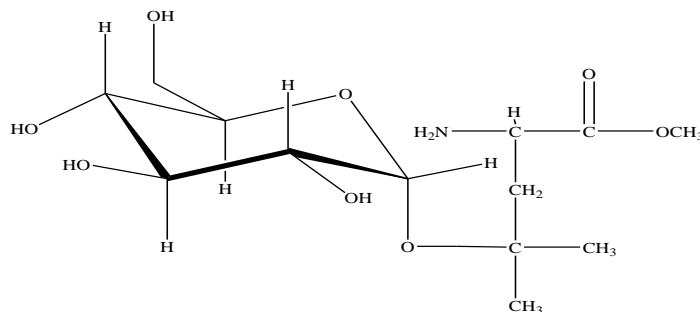
Compound **G** was isolated as insoluble greyish powder with MeOH- $\text{H}_2\text{O}$  (3:1) from Ethyl acetate extract. The  $^{13}\text{C}$  NMR spectrum (see Figure 7) showed 10 signals for 12 carbon atoms from accumulated transient of 912. These were two methyl;  $\delta 17.9$  ppm ( $\text{CH}_3$ ) and  $\delta 23.5$  ppm ( $\text{CH}_3$  branched), a methylene;  $\delta 30.2$  ppm ( $\text{CH}_2$ ) and  $\delta 32.5$  ppm ( $\text{CR}_4$ ), one oxygenated;  $\delta 53.6$  ppm (O-alkyl carbon), a methine;  $\delta 40.4$  ppm ( $\text{CH}$ ) and one carbonyl  $\delta 173.2$  ( $\text{C}=\text{O}$ ) ppm carbon signals respectively. According to the characteristic chemical shifts of the amino acids, the  $^{13}\text{C}$  alpha carbon chemical shift resonances can be assigned to  $\text{C}\alpha$  (40.4 ppm),  $\text{C}\beta$  (32.5 ppm) and  $\text{C}\gamma$  (30.2 ppm). Branched methyl carbon shift is 23.5 ppm while the delta methyl carbon chemical shift is 17.9 ppm. Two methyl groups ( $\delta 17.9$  and  $\delta 23.5$  ppm) are usually coupled to the same  $\text{C}\gamma$ . A leucine residue (2-amino-4-methylpentanoic acid) is contained. The signals  $\delta 62.8$  and 71.8 correspond to (C-6) and (C-2, 3, 5) respectively.

Structure of Glycylglycylglycylglycine (**A**)Structure of  $\alpha$ -D-glucopyranosyl-2-amino-3-methylpentanoic acid (**O**)Structure of  $\alpha$ -D-glucopyranosyl-2-aminomethyl-4-methylpentanoic acid (**E**)

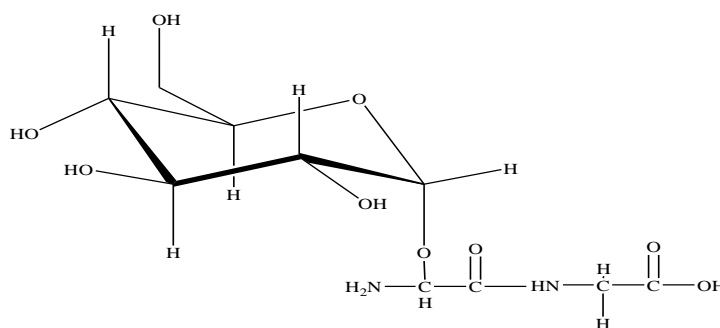
The signal  $\delta$ 101.8(C-1) ppm corresponds to the anomeric signal of a single sugar unit shifted high field and indicated that the carbonyl group is bound to other group. The resonance in the anomeric region in the compound showed the possibility that the carbohydrate unit is single-residue. The chemical shifts of  $\delta$ 62.8, 71.8 ppm correspond to those of carbons 6, 2, 3, 5 respectively of  $\alpha$ -glucopyranose residues. The C-6 signals have shoulders between 74-71 ppm. Chemical shifts of 73-72 ppm are characteristic of  $\alpha$ -D-glucopyranose units. Based on the above results and comparing with published data, **G** were identified as  $\alpha$ -D-glucopyranosyl-2-amino-4-methylmethylpentanoate.

Compound **H** was isolated with H<sub>2</sub>O from 20% acetic acid extract as an insoluble amorphous solid upon repeated chromatography on silica-gel. The <sup>13</sup>C NMR spectrum showed signals of a total of eight signals (Figure 8) for ten carbon atoms from accumulated transient of 976. These were  $\delta$ 20.9 (CH), 30.7(CH), 61.8(C-6), 72.6(C-2, 3, 5), 79.6(C-4), 102.0(C-1), 171.4(C=O) and

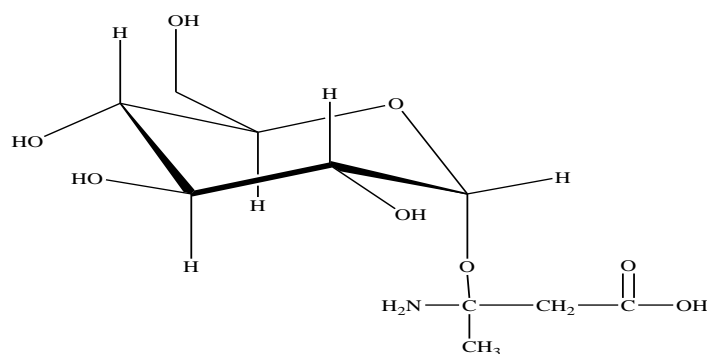
173.4(C=O) ppm. The resonances at 20.9 and 30.7 ppm can be assigned to secondary methylene carbons (-CH-). The  $^{13}\text{C}$  alpha carbon chemical shift is usually, slightly lower than the  $^{13}\text{C}$  alpha carbon chemical shift of other amino acid types. **H** contained the dipeptide (Glycylglycine) residue. Glycine is the only amino acid with only an alpha carbon. The  $^{13}\text{C}$  NMR spectrum confirmed the presence of only one sugar moiety with a single anomeric carbon peak at  $\delta$ 102.0 (C-1) shifted high field due to the attachment to amino acids unit. The signals  $\delta$ 72.6 and 79.6 ppm indicate contribution only from carbons with free hydroxyl groups ('non-linked' carbons, i.e., non-anomeric carbons). The resonances at 102 ppm and 79.6 ppm arose from glycosidic bond carbons C-1 and C-4, respectively. The resonance peak at  $\delta$ 72.6 ppm (C-5 carbons) shifted up field and became a non-resolved shoulder of a resonance C-2, 3 carbons.



Structure of  $\alpha$ -D-glucopyranosyl-2-amino-4-methylmethylpentanoate (**G**)



Structure of  $\alpha$ -D-glucopyranosyl-glycylglycine (**H**)



Structure of  $\alpha$ -D-glucopyranosyl-3-aminobutanoic acid (**I**)

The position of the signal from C-6 atom confirmed pyranose size of the cycle, i.e., single carbohydrate residue present in the compound molecule as single pyranose residue. The

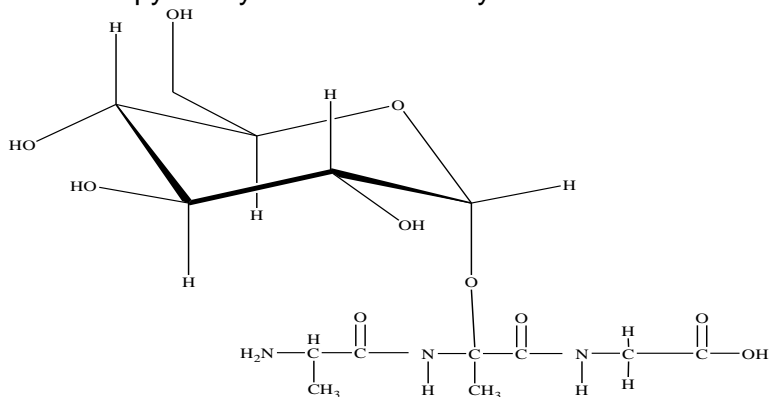
chemical shifts of  $\delta 61.8$  and  $72.6$  correspond to those of carbons 6, 2, 3, 5 respectively of  $\alpha$ -glucopyranose residues. The C-6 signals have shoulders between  $\delta 74$ - $71$  ppm. Chemical shifts of  $\delta 73$ - $72$  ppm are characteristic of  $\alpha$ -D-glucopyranose units. The  $^{13}\text{C}$  NMR data in combination with published data identified **H** as  $\alpha$ -D-glucopyranosyl-glycylglycine with an elemental composition of  $\text{C}_{10}\text{H}_{18}\text{N}_2\text{O}_9$ .

Compound **I** was eluted from crude hexane extract as an insoluble substance with  $\text{H}_2\text{O}$  from a silica gel column. The  $^{13}\text{C}$  NMR spectrum (Figure 9) indicated the presence of  $\delta 16.5$  ( $\text{CH}_2$ ),  $23.7$  ( $\text{CH}_2$ ),  $39.4$  ( $\text{CH}$ ),  $71.1$  (C-2, 3, 5) and  $174.1$  (C=O) ppm from accumulated transient of 1072. The resonance in the anomeric region in the compound showed the possibility that the carbohydrate unit is single-residue (attached to single amino acids units). The position of the signal from C-6 atom confirmed pyranose size of the cycle, i.e., single carbohydrate residue present in the compound molecule as single pyranose residue. The chemical shifts of  $\delta 71.1$  ppm correspond to those of carbons 2, 3, 5 respectively of  $\alpha$ -glucopyranose residues. The C-6 signals have shoulders between  $\delta 74$ - $71$  ppm. Chemical shifts of  $\delta 73$ - $72$  ppm are characteristic of  $\alpha$ -D-glucopyranose units. The  $^{13}\text{C}$  NMR data obtained for the alkyl carbons were similar with **I**. The  $\text{C}\beta$ -carbon ( $\text{CH}$ ) is bonded to  $\text{NH}_2$  will resonate at higher chemical shift  $39.4$  ppm while the  $\text{C}\alpha$  ( $\text{CH}_2$ ) chemical shift is  $23.7$  ppm. The remaining methylene carbon is assigned  $16.5$  ppm. The amino acid residue was identified as a  $\beta$ -alanine (3-aminobutanoic acid). The  $^{13}\text{C}$  alpha carbon chemical shift is usually slightly lower than the  $^{13}\text{C}$  alpha carbon chemical shift of other amino acid types (except glycine). Based on the above results and comparing with published data, **I** was identified as  $\alpha$ -D-glucopyranosyl-3-aminobutanoic acid with an elemental composition of  $\text{C}_{10}\text{H}_{19}\text{NO}_8$ .

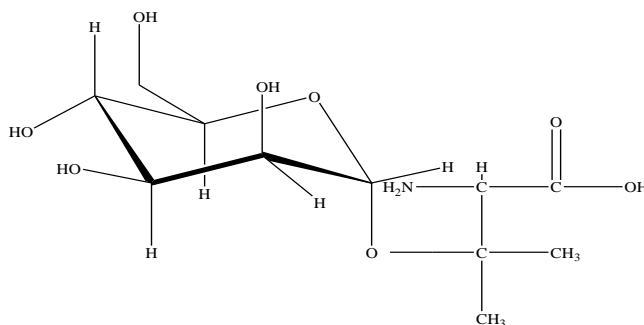
The measured  $^{13}\text{C}$  CP/MAS NMR spectrum of compound **N** isolated as insoluble amorphous milk-white substance with  $\text{H}_2\text{O}$  from unextracted powdered algal biomass is depicted in Figure 10. The accumulated transient is 1088. The peak at  $102.3$  ppm corresponds to C1 carbon in the  $\alpha$ -glycosidic bond, while the signals at  $\delta 177.7$ ,  $182.6$  and  $185.8$  ppm are located in the carbonyl region and can be assigned to two amide group carbons and a carboxylic carbon respectively. The signal at  $\delta 177.7$  and  $182.6$  ppm are shifted to the high field indicating that the carbonyl groups are bound to other groups. The chemical shifts of  $\delta 71.9$  ppm correspond to those of carbons 2, 3, 5 respectively of  $\alpha$ -glucopyranose residues. The C-6 signals have shoulders between  $\delta 74$ - $71$  ppm. The shoulder ( $\delta 71.9$  ppm) observed at the right-hand side of the peak at  $102.3$  ppm is associated with C-1; a single carbohydrate residue. Chemical shifts of  $\delta 73$ - $72$  ppm are characteristic of  $\alpha$ -D-glucopyranose units. Additional peaks observed in the  $^{13}\text{C}$  CP/MAS NMR spectrum were those of aliphatic carbons;  $\delta 23.5$  ( $\text{CH}_2$ ),  $24.5$  ( $\text{CH}_2$ ),  $25.6$  ( $\text{CH}_2$ ),  $39.3$  ( $\text{CH}$ ) and  $41.4$  ( $\text{CH}$ ). The presence of amino acid is confirmed by peaks of carbonyl group (near  $175$  ppm) and peaks of aliphatic carbons (near  $30$  ppm) [54]. The position of the signal from C-6 atom confirmed pyranose size of the cycle. The  $^{13}\text{C}$  NMR spectrum indicated that it is  $\alpha$ -D- glucopyranosyl-2, 4, 6-triamino-4-methylheptanoic acid. The  $^{13}\text{C}$  NMR data in comparison with published data confirmed an elemental composition of  $\text{C}_{14}\text{H}_{25}\text{N}_3\text{O}_{11}$ .

Compound **B** was eluted from a silica gel column with  $\text{H}_2\text{O}$  from methanol extract as an insoluble amorphous substance. The  $^{13}\text{C}$  NMR spectrum (Figure 4) revealed 8 out of 11 carbon atoms from accumulated transient of 1008. Peaks occur at  $\delta 17.3$  ( $\text{CH}_3$ ),  $24.8$  ( $\text{CH}_3$  branched),  $30.8$  ( $\text{CR}_4$ ),  $41.2$  ( $\text{CH}$ ),  $63.1$  (C-6),  $73.4$  (C-2, 3, 5),  $102.2$  (C-1) and  $174.5$  (C=O) ppm. The peak positions of the aliphatic carbon (low-field) resonances are  $\delta 17.3$  and  $24.8$  ppm ( $\text{CH}_3$ ),  $\text{C}\beta$  signal is  $\delta 30.8$  ppm while  $\text{C}\alpha$  bonded to  $\text{NH}_2$  will resonate at  $\delta 41.2$  ppm. The two methyl groups ( $17.3$  and  $24.8$  ppm) are usually coupled to the same beta carbon ( $\delta 41.2$  ppm). The peak centred at  $174.5$  ppm in the  $^{13}\text{C}$  CP-MAS spectrum can be assigned to the only carbonyl carbon present in the molecule, the amide linkage of the amino acid moiety. The amino acid residue was identified as valine (2-amino-3-methylbutanoic acid). Signal at  $73.4$  ppm are due to C2, C3, and C5. The

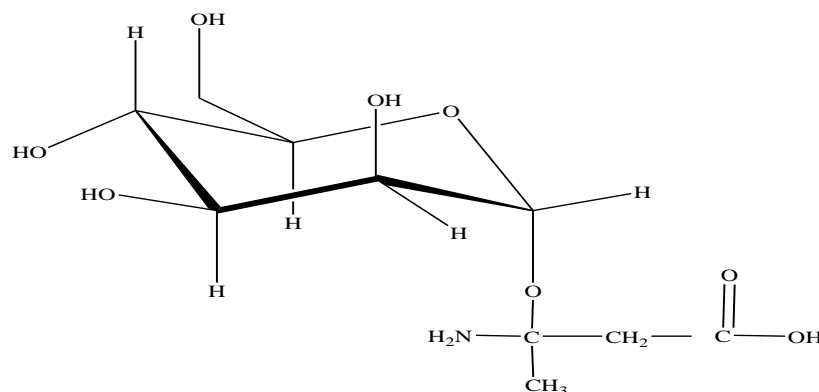
peak centred at 102.2 ppm is due to anomeric C-1 of glucose fragment in a carbohydrate. The resonance in the anomeric region in the compound showed the possibility that the carbohydrate unit is single-residue. The position of the signal from C-6 atom confirms pyranose size of the cycle. The chemical shifts of  $\delta$ 73.3, 63.1 ppm correspond closely to those of carbons 2, 3, 5 and 6, respectively, of  $\alpha$ -D-mannopyranose units. The signals have shoulders between  $\delta$ 76-68 ppm. The position of mannopyranosyl signal suggested  $\alpha$ -configuration of the anomeric centre, which is confirmed by the chemical shift value of its C-1 atom in the region of  $\delta$ 102 ppm. The signal position from the C-6 in unsubstituted mannose residues ( $\delta$ 62.0 ppm) demonstrated a pyranose size of the mannose cycle. Note that mannose atoms C-1, C-4 and C-6 are involved in the formation of covalent bonds, which causes the shift in their signals to weak field. Based on the above results and comparing with published data, **B** had elemental composition of  $C_{11}H_{21}NO_8$  and identified as  $\alpha$ -D-mannopyranosyl-2-amino-3-methylbutanoic acid.



Structure of  $\alpha$ -D-glucopyranosyl-2, 4, 6-triamino-4-methylheptanoic acid (**N**)



Structure of  $\alpha$ -D-mannopyranosyl-2-amino-3-methylbutanoic acid (**B**)



Structure of  $\alpha$ -D-mannopyranosyl-3-aminobutanoic acid (**D**)

Figure 5 showed the solid state  $^{13}\text{C}$  NMR (CPMAS) spectrum of **D** isolated with MeOH- $\text{CHCl}_3$  (80:20) from methanol extract as an insoluble sticky amorphous substance. The  $^{13}\text{C}$  NMR chemical shifts include  $\delta$ 16.9 ( $\text{CH}_2$ ), 24.1 ( $\text{CH}_2$ ) and 38.7 ( $\text{CH}$ ) ppm which are assigned to saturated alkyl carbons of the aliphatic amino acid [55]. The accumulated transient is 1008. The signals at  $\delta$ 16.9 indicate  $\text{C}_\gamma$ , 24.1 is  $\text{C}_\alpha$  while 38.7 is  $\text{C}_\beta$ . Carbonyl carbon ( $\text{C}=\text{O}$ ) in the peptide bond is  $\delta$ 174.7 ppm. The residue amino acid in **D** is  $\beta$ -alanine (3-aminobutanoic acid). Peaks in the region 58–110 ppm are mostly due to carbohydrate. Peaks at  $\delta$ 73.2 indicate C-2, 3, 5 while signal at  $\delta$ 101.7 is the anomeric carbon (C-1). The resonance in the anomeric region in the compound showed the possibility that the carbohydrate unit is single-residue. The chemical shifts of  $\delta$ 73.2 ppm correspond closely to those of carbons 2, 3, 5 respectively, of  $\alpha$ -D-mannopyranose units. The signals have shoulders between  $\delta$ 76-68 ppm. The position of mannopyranosyl signal suggested  $\alpha$ -configuration of the anomeric centre, which is confirmed by the chemical shift value of its C-1 atom in the region of  $\delta$ 102 ppm. The signal position from the C-6 in unsubstituted mannose residues ( $\delta$ 62.0 ppm) demonstrated a pyranose size of the mannose cycle. Mannose atoms C-1, C-4 and C-6 are involved in the formation of covalent bonds, which caused the shift in their signals to weak field. The  $^{13}\text{C}$  NMR data in combination with published data, confirmed an elemental composition of  $\text{C}_{10}\text{H}_{19}\text{NO}_8$  for **D** identified as  $\alpha$ -D-mannopyranosyl-3-aminobutanoic acid.

## V. Conclusion

The present study was to isolate and characterise some bioactive compounds in freshwater microalgae. This study resulted in the isolation and characterization of glycoamino acids. Of the nine compounds isolated from microalgae, eight have a glycan skeleton with attached amino acids units. These are not very common metabolites but hold promise as drug leads. The compounds were found to be active when tested with microbes indicating that microalgae could be a preservative in feeding manufacturing. This work indicates that microalgae have the potential to enhance the diversification of the Nigerian aquaculture industry with its composition of compounds that could be used in feed preservation and as multivalent scaffolds for projecting pharmacophore groups. Today the world is faced with devastating ailments such as malaria, cancer, diabetics and tuberculosis, and biological resources such as microalgae might provide solution to this misery.

## VI. References

1. Ogbonna, J. C.; Yoshizawa, H. & Tanaka, H. Treatment of high strength organic wastewater by a mixed culture of photosynthetic microorganisms *Journal of Applied Phycology*, 12(2000) 277-284.
2. Thidarat Papone, Supaporn Kookkhunthod and Ratanaporn Leeing *International Journal of Biological, Biomolecular, Agricultural, Food and Biotechnological Engineering*, 6(2012):195-199
3. Anon. Mixed cultivation of *Euglena gracilis* and *Chlorella sorokiniana*: a production method of algae biomass on a large scale. *Journal of Applied Biosciences* 35(2010). 2225 – 2234
4. Olaizola, M. Commercial development of microalgal biotechnology: from the test tube to the market place. *Biomolecular Engineering*, 20(2003)459-466
5. Singh, S.; Kate, B. N. & Banecjee, U. C. Bioactive compounds from cyanobacteria and microalgae: an overview. *Critical Reviews in Biotechnology* 25(2005)73–95
6. Boyd, C.E. *Water Quality in Warm Water Fish Ponds*. Agricultural Experiment Station. Auburn University, Alabama, USA. 2000.
7. Yamagishi, T. *Plankton Algae in Taiwan (Formosa)*. Uchida Rokakuku, Tokyo, Japan. (1992) 253 pp.
8. Vymazal, J. *Algae and Element Cycling in Wetlands*. CRC Press, Inc., Boca Raton, Florida, USA. (1995)689 pp.
9. Ciferri, O. *Spirulina, the Edible Micro-Organism*. *Microbiological Reviews*, 47(1983). 551-578.
10. Tomaselli, *Morphology, Ultrastructure and Taxonomy of Arthrospira (Spirulina) maxima and Arthrospira (Spirulina) platensis*. In: A. Vonshak, Ed., *Spirulina platensis (Arthrospira): Physiology, Cell-Biology and Biotechnology*, Taylor and Francis, London, 1997, 1-16.
11. Ballot, A.; Dadheech, P. and Krienitz, L. Phylogenetic Relationship of *Arthrospira*, *Phormidium*, and *Spirulina* strains from Kenyan and Indian Water bodies, *Agra University Journal of Research: Science*, 113(2004)37-56.
12. Gomont, M. M. *Monographie des Oscillariées (Nostocacées Homocystées)*. *Ann. Sci. Nat. Bot., Ser. 7*(1892). 263-368.
13. Anagnostidis, K. and Golubic, S. *Über die Ökologie einiger Spirulina-Arten*. *Nova Hedwigia* 11(1966). 309-335.
14. Guglielmi and C. Bazirge (1982). *Structure et Distribution des pores et des Perforations de l'enveloppe de Peptidoglycane chez Quelques Cyanobactéries*. *Protistologica*, 18:151-165.
15. Rethmeier, J. "Untersuchungen zur Ökologie und zum Mechanismus der Sulfidadaptation mariner Cyanobakterien der Ostsee," PhD Thesis, (1995).
16. Komárek, J. *Diversita a Moderní Klasifikace Sinic (Cyanoprokaryota) Diversity and Modern Classification of Cyanobacteria (Cyanoprokaryota)*. Inaugural Dissertation Not Published, (1992).
17. Zhu, W.; Chiu, M. C. L.; Ooi, V. E. C.; Chan, P. K. S. & Angjr, O. P. Antiviral property and mode of action of a sulphated polysaccharide from *Sargassum platens* against herpes simplex virus type 2. *International Journal of Antimicrobial Agents*, 24(2004)18-25
18. Conte, P.; Piccolo, A.; van Lagen, B.; Buurman, P. & Hemminga, M. A. Effects of residual ashes in CP-MAS 13C-NMR spectra of humic substances from volcanic soils. *Fresenius Environmental Bulletin*, 10(2001)369–374.

19. Mao, J. D. & Schmidt-Rohr, K. Separation of acetal or ketal O–C–O <sup>13</sup>C NMR signals from aromatic-carbon bands by a chemical shift-anisotropy filter. *Solid State NMR* 26(2004). 36–45. doi:10.1016/j.ssnmr.2003.09.003
20. Wilson, M. A. *NMR techniques and applications in geochemistry and soil chemistry*. Pergamon Press Oxford (UK), 1987
21. Schofield, J. D. and Baianu, I. C. *Cereal Chemistry* 1982, 59240–245
22. Roscoe, R.; Buurman, P. and Van Lagen, B. *Bras Ci Sol*; 2004, 28: 811-18
23. Skjemstad, J. O; Frost, R. L.; Barron, P. F. *Australian Journal of Soil Science*, 1983, 21: 539-47.
24. Lemma, B.; Nilsson, I.; Kleja, D. B.; Olsson, M. and Knicker, H. *Soil Biology and Biochemistry*; 2007, 39: 2317-28.
25. Quideau, S. A.; Chadwick, O. A.; Benesi, A.; Graham, R. C. and Anderson, M. A. *Geoderma*; 2001, 104: 41-60.
26. Keenan, M. H. J.; Belton, P. S.; Matthew, J. A. and Howson, S. J. *A Carbohydrate Research* 1985, 138:168–170.
27. Renard, C. M. G. C. and Jarvis, M. C. *Carbohydrate Polymer*, 1999, 39:209–216
28. Maunu, S.; Liitiä, T.; Kauliomäki, S.; Hortling, B. and Sundquist, J. *Cellulose*; 2000, 7:147-59.
29. Taylor, R. E., French, A. D. and Gamble, G. R. *Journal of Molecular Structure* 2008, 878:177-84.
30. Sinitsya, A.; Čopikova, J.; Prutyánov, V.; Skoblya, S. and Machovic, V. *Carbohydrate Polymer*, 2000, 42: 359–368.
31. Malovikova, A. and Kohn, R. *Czech. Chem. C.*, 1986, 51: 2259–2270
32. Jarvis, M. C. and Apperley, D. C. *Carbohydrate Research* 1995, 275: 131.
33. Sinitsya, A.; Čopikova, J. and Pavlikova, H. *Journal Carbohydrate Chemistry*, 1998, 17: 279–292.
34. Rajamohanam, P. R.; Ganapathy, S.; Vyas, P. R.; Ravikumar, A. and Deshpande, M. V. (1996). *Journal of Biochemical and Biophysical Methods*, 1996, 313(4):151–163
35. van de Velde, K. and Kiekens, P. *Carbohydrate Polymers*, 2004, 584:409–416
36. Muhammad Saad Shaikh; Simon Rawlinson and Natalia Karpukhina A. *Pakistan Oral and Dental Journal* 2014, 34:2
37. Carlsson, A. S.; van Beilen, J. B.; Moller, R. and Clayton, D. *Micro- and Macro-Algae: Utility for Industrial Applications* 1st ed. Newbury: CPL Press, 2007
38. Borowitzka, M. A. *Algal Culturing Techniques*. Burlington, MA: Elsevier Academic Press; 2005
39. Van Gerpen, J. H. and He, B. *Thermochemical Conversion of Biomass to Liquid Fuels and Chemicals*, 2010, 382-415.
40. Halim, R.; Gladman, M.; Danquah, and P. Webley. *Bioresource Tech.* 2011, 102(1): 178-185
41. Liu, J.; Huang, J.; Sun, Z.; Zhong, Y.; Jiang, Y. and Chen, F. *Bioresource Technology*, 2011, 102(1):106-110.
42. Desbois, P. A.; Spragg, A. M. & Smith, V. J. A Fatty Acid from the Diatom *Phaeodactylum tricornutum* is Antibacterial against Diverse Bacteria Including Multi-resistant *Staphylococcus aureus* (MRSA). *Marine Biotechnology*, (2008)1436-2236
43. Shin, S. Y.; Bajpai, V. K.; Kim, H. R. & Kang, S. C. Antibacterial activity of eicosapentaenoic acid (EPA) against foodborne and food spoilage microorganisms, *Food science and Technology*, 40(2006)1515



44. Mengesha, A. E. Isolation, Structural Elucidation, Quantification and Formulation of the Saponins and Flavonoids of the Seeds of *Glinus Lotoides*. PhD Dissertation der Fakultät für Chemie und Pharmazie der Eberhard-Karls-Universität Tübingen zur Erlangung des Grades eines Doktors der Naturwissenschaften, (2005)194 pages
45. Fyfe, C. A. Solid state NMR for chemists. C.F.C. Press, Guelph, Ont, 1984.
46. Ross, C.; Beier, B.; Radford, P.; Mundy and Garya Strobel Canadian Journal of Chemistry, 1980, 58:2800
47. Bock, K. and Pedersen, C. Advances in Carbohydrates Chemistry and Biochemistry, 1983, 41:27-66
48. Kamide, K.; Okajima, K.; Kowsaka, K. & Matsui, T. CP-MAS <sup>13</sup>C-NMR Spectra of Cellulose Solids: An explanation by the intramolecular Hydrogen Bond Concept. Polymer Journal 17(1984):701-706
49. Yuki, G. K. NMR studies on carbohydrates - Application of <sup>13</sup>C NMR to determine composition, conformation, and dynamics of polysaccharides. Journal of Synthetic Organic Chemistry, Japan, 37(1979.):935-947
50. Majerle, A.; Kidric, J. and Jerala, R. Journal of Antimicrobiology and Chemotherapy. 2003, 51: 1159-1165.
51. Kricheldorf, H. R.; Muller, D. & Ziegler, K. Carbon-13 NMR CP/MAS investigation of silk proteins. Polymer Bulletin 9 (1983)284–291.
52. Kricheldorf, H. R. & Muller, D. Characterisation of proteins by means of C-13 NMR CP/MAS spectroscopy. Colloid and Polymer Science 262(1984) 856–861.
53. Wamer, I & Witkowski, S. Analysis of solid state <sup>13</sup>C NMR of biologically active compounds. Current organic chemistry, 5(2001)987-999
54. Diaz, L. E.; Morin, F.; Mayne, C. L. & Grant, D. M. Magnetic Resonance Chemistry, 24(1986)167
55. Conte, P; Piccolo A.; van Lagen, B.; Buurman, P. and Hemminga, M. A. Solid State Nuclear Magnetic Resonance, 2002, 21:158–17
56. Synytsya, A.; Čopíková, J.; Prutyánov, V.; Skoblyá, S. and Machovic, V. Carbohydrate Polymers, 2009, 76(4):548–556

**Please cite this Article as:**

Emeka Ugoala, George Ndukwe, Rachael Ayo, Isolation and Characterisation of Some Microalgae Bioactive Molecules, ***Algerian J. Nat. Products*, 4:3 (2016) 323-347.**

www.univ-bejaia.dz/ajnp

Online ISSN: 2353-0391

Editor in chief: Prof. Kamel BELHAMEL

Access this article online	
Website: <a href="http://www.univ-bejaia.dz/ajnp">www.univ-bejaia.dz/ajnp</a>	Quick Response Code
DOI: <a href="https://doi.org/10.5281/zenodo.200210">https://doi.org/10.5281/zenodo.200210</a>	